THE JOURNAL OF PHYSICAL CHEMISTRY C
A JOURNAL OF THE AMERICAN CHEMICAL SOCIETY

pubs.acs.org/JPCC

Article

Atomically Precise Palladium Nanoclusters with 21 and 38 Pd Atoms Protected by Phenylethanethiol

Senthil Kumar Eswaramoorthy and Amala Dass*

Cite This: J. Phys. Chem. C 2022, 126, 444−450

Read Online

ACCESS | Metrics & More | Article Recommendations | Supporting Information

ABSTRACT: Monolayer thiolate-protected nanoclusters (MPCs) are extensively studied due to their distinctive properties. The atomic precision in MPCs, especially in gold MPCs, is determined through mass spectrometry, which leads to the accurate identification of metal-ligand composition. The total structure determination of gold and silver MPCs using ScXRD revolutionized the field by providing insights into the structural arrangement at an atomic level. The synthesis of atomically precise MPCs using other metals like palladium (Pd) to study and compare properties is tedious and complex. In one end, larger size monodisperse Pd nanoparticles (NPs) were synthesized and studied for various catalytic properties. Meanwhile, on the other end, a small-molecule tiara-like Pd−thiolate complex was reported. However, atomic precise Pd MPCs in the middle and its detailed studies are not yet explored. Here, we report the synthesis and identification of atomically precise phenylethanethiol-protected $Pd_{21}(SCH_2CH_2Ph)_{18}$ and $Pd_{38}(SCH_2CH_2Ph)_{21}S_2$ Pd nanoclusters. The size distribution is confirmed using matrix-assisted laser desorption ionization mass spectra (MALDI-MS), and electrospray ionization mass spectrometry (ESI-MS) confirms the composition through the isotopically resolved peak. The X-ray photoelectron spectroscopy (XPS) spectra elucidate the cluster formation in smaller size.

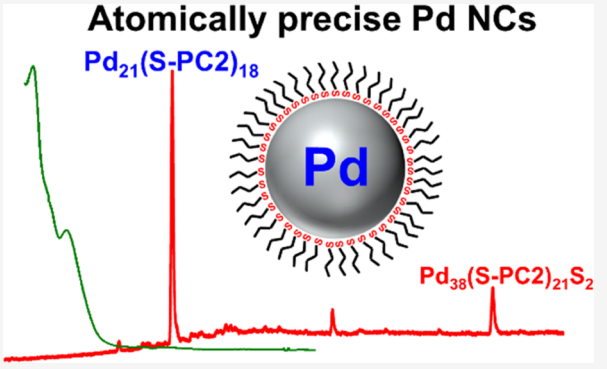

INTRODUCTION

Monolayer thiolate-protected nanoclusters (MPCs) composed of a metal core with sizes ranging from tens to thousands of atoms are extensively studied in recent years due to their distinct optical, electronic, and catalytic properties.[1−3] In thiolate-protected metal nanoclusters, atomic precision is achieved through thermochemical etching.[1,4−8] The unique properties arise from the quantum size effects which leads to a wide range of applications in catalysis, sensing, energy, targeted drug delivery, and solar cells.[9−18]

High-resolution transmission electron microscopy (HR-TEM) was commonly used to study gold nanoparticles (Au NPs), but smaller clusters suffered from beam damage. The introduction of mass spectrometry to characterize Au NPs changed the course of the field. In the beginning, laser desorption ionization mass spectrometry (LDI-MS) combined with HR-TEM elucidated the discovery of quantitatively separable gold nanocrystal.[1,2,4−6,19−21] Then, matrix-assisted LDI-MS (MALDI-MS) produced mass spectra with minimal fragmentation.[22−24] Later, by choosing a suitable organo-soluble matrix and using threshold laser intensity, fragment-free molecular peaks were achieved in MALDI-MS.[25]

The introduction of electrospray ionization mass spectrometry (ESI-MS)[26,27] on MPCs resulted in the ionization of intact cores with no fragmentation.[17,28,29] Especially for gold MPCs, the soft ionization technique of ESI-MS provided the MPC composition with atomic precision.[30] Initially, the atomic composition of various glutathione-protected gold clusters were determined using ESI-MS by Tsukuda and co-workers.[31−34] Then, the composition of the well-studied $Au_{25}(SC_2H_4Ph)_{18}$ was determined by Murray group.[28] Finally, isotopically resolved ESI-MS data of the same $Au_{25}(SC_2H_4Ph)_{18}$ cluster that exactly matched the theoretically calculated spectra confirmed the atomic precision beyond any doubt.[30] Later, the total structure of $Au_{25}(SC_2H_4Ph)_{18}$ determined using single-crystal X-ray diffraction (ScXRD) confirmed the exact number of gold atoms and thiolate ligands, previously determined using ESI-MS.[35]

In noble metal MPCs, gold MPCs were the most studied and well-established systems, followed by silver MPCs.[36−42] Recently, few studies on copper MPCs were reported.[43,44] The study of other metals, particularly with thiolate-protected clusters, is minimal. Palladium (Pd) metal is known for its high catalytic activity in both homogeneous and heterogeneous catalysis.[45,46] The 2010 noble prize awarded to Pd-catalyzed Suzuki cross couplings in organic synthesis explains the

Received: November 1, 2021
Revised: December 3, 2021
Published: December 22, 2021

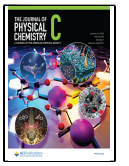

https://doi.org/10.1021/acs.jpcc.1c09453
J. Phys. Chem. C 2022, 126, 444−450

importance of Pd in catalysis.[47] The Suzuki coupling uses Pd salts or organopalladium complexes. Meanwhile, 11-mercaptoundecanoic acid-covered Pd NPs can be reused several times for the same Suzuki coupling reaction.[48]

Dahl and Mednikov explored in detail the formation of Pd nanoclusters with carbonyl/phosphine ligands ($Pd_n(CO)_x(PR_3)_y$).[49−51] There are ∼19 distinct Pd core geometries, with core Pd atoms ranging from 10 to 165, that have been isolated and structurally determined using ScXRD. The Pd forms a highly condensed carbonyl/phosphine ligand nanocluster that exhibits unprecedented geometrical diversity of icosahedral or closed cubic/hexagonal closed packing-based metal core geometries.[50] It is important to note that these Pd nanoclusters are only stable in inert conditions. While the relatively weak metal−metal and metal−CO bonds lead to a large number of $Pd_n(CO)_x(PR_3)_y$ clusters with structural diversity,[49] weaker bonds result in unstable compounds and are therefore not well studied when compared with thiolated Au nanoclusters.

On the other hand, Pd nanoparticles protected by thiolate ligands make a good candidate for various catalysis. The thiolate-protected Pd NPs showed excellent catalytic activity in Heck reaction.[47] In a study where n-alkanethiol self-assembled monolayer (SAM) was coated on the Pd surface, the selectivity of 1-epoxybutane formation from 1-epoxy-3-butene improved from 11 to 94%.[52]

An understanding of the chemical composition and structural arrangements of thiolate-protected Pd NPs is essential to understand their properties. Pd NPs were characterized using transmission electron microscopy (TEM) before.[53,54] However, TEM data provides only size distribution where 1 nm difference provides a difference of hundreds of atoms. Various water and organic-soluble small Pd NPs like Jin et al. work on $Pd_{13-17}(SR)_{18-22}$ (R = Ph-tBu),[53] Choi and collaborators work on a series of water-soluble *N*-acetyl-L-cysteine-protected ultrasmall Pd NPs,[55] and Tsukuda et al. work on a range of $Pd_n(SR)_m$ clusters ($5 \leq n \leq 60$) with $m \sim 0.6$ n[54] were reported using MALDI-MS characterization.[53−55] However, due to its hard ionization, MALDI-MS could provide an approximate composition of metal atoms and protecting ligands.[22−24,53−55]Tiara-like Pd complexes with formula ($Pd_n(SR)_{2n}$), where n = 2−20, were reported with atomic precision and ScXRD structure.[56−63] However, they are not Pd nanoclusters having a metal core and surface ligands. Therefore, to fulfill the prerequisite and modulate the properties of thiolate-protected Pd NPs, atomic precise Pd MPCs need to be synthesized and identified. ESI-MS, due to its soft ionization, is one of the main tools to identify atomic precision, which leads to the identification of chemical composition.

In this work, we report atomically precise palladium nanoclusters with 21 and 38 Pd atoms protected by phenylethanethiol confirmed using isotopically resolved ESI-MS. MALDI-MS confirms the size distribution and UV−vis spectra confirm the molecular nature.

METHODS

Materials. Palladium(II) chloride 99.9% (metal basis) Pd 59.0% (Alfa Aesar), tetra-*n*-octylammoniumbromide (ToABr, Acros, 99%), hydrochloric acid (ACS grade) (VWR), sodium borohydride (Acros, 99%), phenyl-ethanemercaptan (Sigma-Aldrich), and trans-2-[3-(4-tertbutylphenyl)-2-methyl-2-propenylidene]malononitrile (DCTB matrix) (Fluka ≥ 99%) were used as received. High-performance liquid chromatography (HPLC) grade solvents such as tetrahydrofuran, toluene, methanol, butylated hydroxytoluene-stabilized tetrahydrofuran, and acetonitrile were obtained from Fisher Scientific. Bio-Rad-SX1 beads (BioRad) were used for size exclusion chromatography.

Instrumentation. MALDI mass spectra were acquired using Voyager-De PRO MALDI-time of flight mass spectrometry using DCTB[25] matrix. ESI mass spectra were collected using Waters Synapt XS instrument, with tetrahydrofuran as a solvent. UV−visible absorption spectra were collected using a Shimadzu UV-1601 instrument, and samples were dissolved in toluene.

Synthesis. Pd nanoclusters were synthesized based on a modified synthetic protocol reported in literature.[64,65] In this procedure, first, a crude product was synthesized based on Brust two-phase synthesis.[65] Then, the crude was thermochemically treated with increased temperature, and finally, the pure product was isolated using size exclusion chromatography (SEC).[66]

Crude Synthesis. Palladium chloride ($PdCl_2$) (0.1 g) was dissolved in 0.366 mL of concentrated hydrochloric acid and 1.5 mL of H_2O. ToABr (0.47 g) was dissolved in 5 mL of toluene separately. They are both mixed in a 100 mL round-bottom flask under stirring at 500 rpm. The mixture was allowed to stir for 15 min. When phase transfer was completed, the organic layer was separated and 57 mL of phenylethanethiol (PC2) (Pd/Thiol = 1:0.75) was added. Then, the reaction between gold and thiol was allowed for 1 h with the same stirring rate. At this point, the reaction was reduced by rapidly adding 0.2 g of $NaBH_4$ (Pd/$NaBH_4$ = 1:10) dissolved in 5 mL of ice-cold water. The solution changed to black color indicating the formation of nanoclusters. The stirring was continued for about 18 h. Then, the resulting product's organic phase was separated, and the rotary evaporated to remove excess solvent. Finally, the product was washed with excess methanol−water mixture to obtain the crude.

Etching and SEC. The washed crude product, ∼130 mg, was thermochemically treated (etching) at 70 °C with 2.5 mL of toluene and 2.5 mL of excess PC2 thiol for 24 h. The etched product was rotary evaporated and washed with methanol and water mixture to remove all of the byproducts. The final step was to isolate the different sizes of the product using SEC. When the etched product was passed through the SEC column, two differentiable bands (yellow and dark) were seen. These two bands represent two completely different products with a significant mass difference. The reported Pd nanoclusters were obtained from the yellow band.

RESULTS AND DISCUSSION

Pd nanoclusters are synthesized using a modified method of two-phase Brust synthesis.[65] The step-by-step synthesis process is explained in the experimental section. Briefly, the Pd salt was dissolved in water with the help of conc. HCl, then phase transferred to toluene using ToABr, followed by the addition of thiol, and finally reducing the mixture using an aqueous solution of $NaBH_4$ forming the crude. The crude is then etched and purified using SEC. In general, the identification of nanoclusters (NCs) other than Au NCs with mass spectrometry is a challenge. However, by the experience gained by our group to obtain mass spectrometry data on difficult larger Au NCs, we were able to obtain ESI-MS data of the atomically precise Pd NCs shown in Figure 1. As

https://doi.org/10.1021/acs.jpcc.1c09453
J. Phys. Chem. C 2022, 126, 444−450

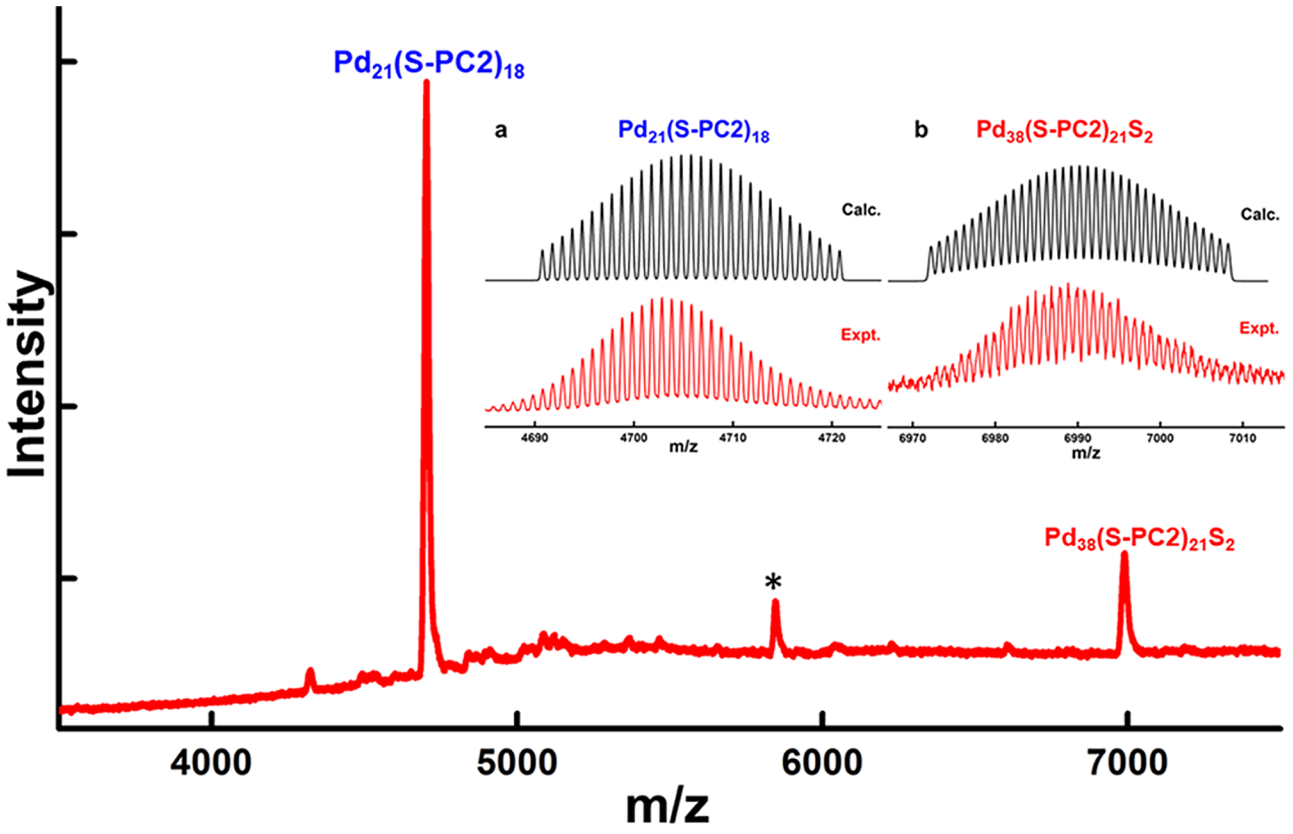

Figure 1. Electrospray ionization mass spectra (ESI-MS) of the size exclusion chromatography (SEC)-purified product of Pd nanoclusters protected by phenylethanethiol (PC2) showing two products, $Pd_{21}(SR)_{18}$ and $Pd_{38}(SR)_{21}S_2$. *Represents less intense peak at 5844 Da. Insets: (a) comparison of the experimental and theoretical spectrum of $Pd_{21}(SCH_2CH_2Ph)_{18}$ and (b) comparison of the experimental and theoretical spectrum of $Pd_{38}(SCH_2CH_2Ph)_{21}S_2$.

mentioned in the experimental section, the first part of the synthesis provides a crude product, which was then reacted with excess thiol at elevated temperature to obtain an etched product with narrow size distribution. The etched product was purified using size exclusion chromatography (SEC).

Figure 2 shows the MALDI-MS spectra of selected SEC fractions. Fraction 8 (F08) represents the yellow band and fraction 4 (F04) represents the dark band. A photograph of the SEC column is shown on the right in Figure 2. The SEC column has two major bands, yellow and dark bands. Their corresponding MALDI-MS spectrum in positive mode is shown on the left side of Figure 2. The top spectrum corresponding to the yellow band displays many sharp peaks below 5 kDa. The sharp peak represents the atomic precision of NCs. In other words, these NCs are precise enough to ionize in ESI-MS. MALDI-MS is a hard ionization technique, where the ionization is caused by ablation of a sample using a laser. So, NCs tend to fragment in MALDI-MS, which corresponds to the multiple peaks in the top spectra. In comparison, ESI-MS is a soft ionization technique that is more important to identify the molecular mass of NCs. The bottom spectrum corresponds to the dark band showing a broad peak from 4 to 14 kDa. Since the dark band has a broad peak, it was not ionizing, and no peaks were observed in the ESI-MS.

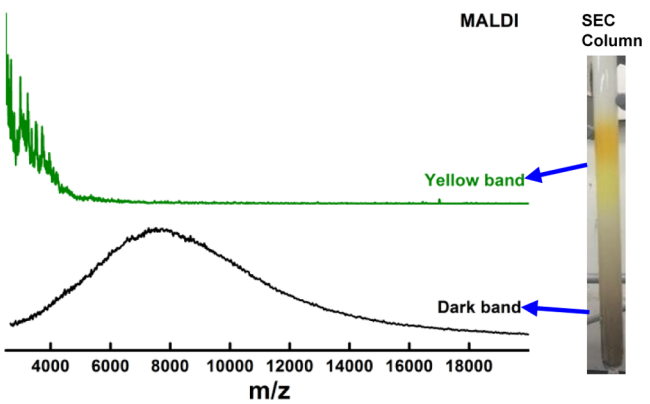

Figure 2. Matrix-assisted laser desorption ionization mass spectra (MALDI-MS) of size exclusion chromatography (SEC) products; in that, the top spectra correspond to the yellow band, which has low mass products. The bottom spectra come from the dark band, which has high mass products compared to the yellow band.

The ESI-MS in positive mode of SEC-purified product as shown in Figure 1 has two major peaks, which are identified as 4700 and 6989 Da. An expanded view of these two peaks is shown in Figure 1(inset). The NCs are formed with a metal core that is protected by thiolate ligands.

These NCs have a precise number of metal and ligand count, Pd_xSR_y, where x and y represent the number of Pd atoms and ligands, respectively, in the NC. In some cases, sulfur atoms alone can bond with a metal core in the absence of a ligand chain and can be denoted as $Pd_xSR_yS_z$.[67] The NC at 4700 Da is identified as $Pd_{21}(SCH_2CH_2Ph)_{18}$, and 6989 Da is identified as $Pd_{38}(SCH_2CH_2Ph)_{21}S_2$. Figure 1(inset) shows an expanded view of the major peaks revealing the isotopic distribution of these two NCs. The bottom spectrum of Figure

https://doi.org/10.1021/acs.jpcc.1c09453
J. Phys. Chem. C 2022, 126, 444−450

1a is an expanded view of Figure 1 at 4700 Da range to show the isotopic distribution of NC. The isotopomer splitting showing (Figure 1a,b) mass difference of 1 Da suggests that these peaks correspond to the 1 + charge state of the respective Pd NCs. The top spectrum of Figure 1a is a calculated spectrum of $Pd_{21}(SCH_2CH_2Ph)_{18}$ with isotopically resolved peaks. The exact match between the experimental and theoretical spectra confirms the composition that the NC has 21 Pd atoms protected by 18 thiolate ligands. Likewise, in Figure 1b, the top spectrum is a calculated spectrum of $Pd_{38}(SCH_2CH_2Ph)_{21}S_2$ and the bottom spectrum is an expanded view of Figure 1 at 6989 Da range. The isotopic matching of theoretical and experimental spectra confirms the assigned chemical composition. The less intense peak at 5844 Da is not isotopically resolved to exactly assign the peak. The closest match of the 5844 Da peak is $Pd_{34}(SCH_2CH_2Ph)_{16}S$. Previously reported studies on thiolate-protected larger Pd NCs and thiolate SAM on the 2D Pd surface suggest that the formation of a Pd−S interlayer between the core and thiolate ligand adds stability.[68−70]

The UV−vis spectra, Figure 3, correspond to the SEC-purified yellow band product from F08. The inset of Figure 3

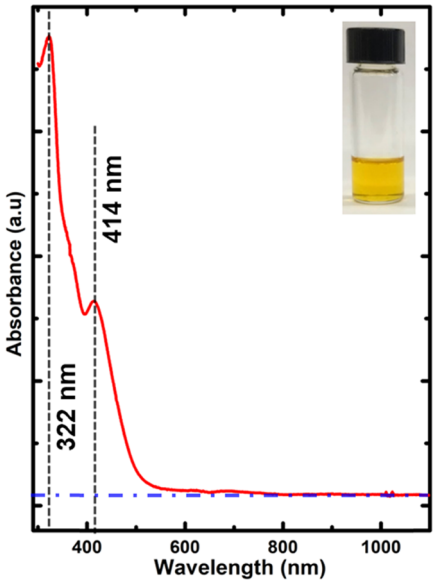

Figure 3. Ultraviolet and visible (UV−vis) spectra of the size exclusion chromatography (SEC)-purified product of Pd nanoclusters protected by phenylethanethiol (PC2) in toluene. The blue dash-dot line represents the baseline.

shows the photograph of the SEC-purified yellow band sample in toluene. The UV−vis spectra show two distinct features, ~414 and ~322 nm, rise from ~600 nm. These two features are close to the reported $Pd_6(SC_{12}H_{25})_{12}$ complex.[55,58,71] The ESI-MS comparison of fractions 8−10 (Figure S1) shows that most of the smaller complexes eluted in the latter fractions (F09 and F10), and minute amounts remain in fraction 8. In the seminal work of Negishi et al., on 1 nm Pd clusters, a similar optical spectrum was reported.[54] Though they observed features of the $Pd_6(SR)_{12}$ complex, based on several factors, they ascribe that a significant portion of the spectrum contributed by $Pd_n(SR)_m$ clusters. Similarly, based on the ESI-MS data (Figure S1), X-ray photoelectron spectroscopy (XPS) data (Figures 4, S2, and S3), and the SEC separation technique, we can ascribe that a significant portion of the spectrum is from Pd NCs.[54]

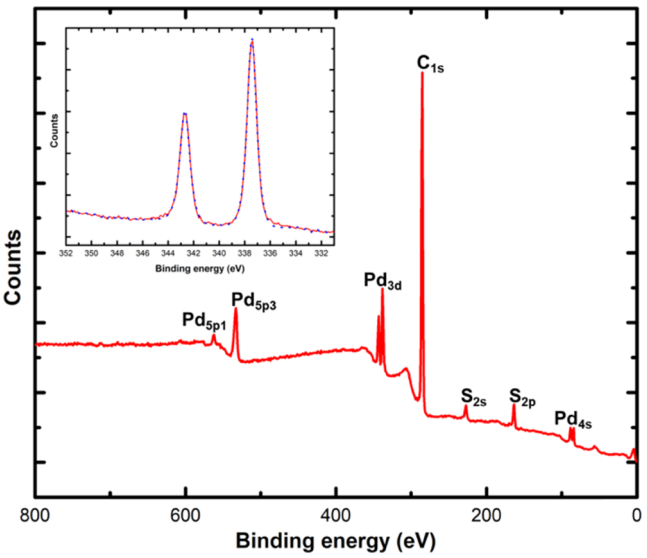

Figure 4. X-ray photoelectron spectroscopy (XPS) spectrum of the SEC-purified product of Pd nanoclusters protected by phenylethanethiol. Inset: a high-resolution spectrum focused on the Pd 3d region.

The full survey X-ray photoelectron spectrum (XPS) of SEC-purified Pd NCs (yellow band) with the main core-level lines is presented in Figure 4. Here, the spectral features corresponding to palladium (Pd), sulfur (S), and carbon (C) are detected. The XPS spectrum is calibrated using C 1s photoemission at 285 eV. XPS features of all elements of the clusters with their photoelectron shell identification are shown in Figure 4, and their high-resolution core-level spectra are shown in Figure S2. The high-resolution Pd core-level photoemission spectra (Figure 4(inset)) show two peaks: 342.6 and 337.3 eV, which have been assigned as Pd $3d_{3/2}$ and Pd $3d_{5/2}$ of Pd clusters. The Pd $3d_{5/2}$ peak position at 337.3 eV is located between Pd metal (335.1 eV) and Pd(II) in $PdCl_2$ (338 eV).[72−74] The observation of these features for these clusters is qualitatively interpreted based on XPS studies on gold nanoclusters.[32,75−77] In these studies, monotonic shift of the Au($4f_{7/2}$) peak is observed due to two components: "final state effect" arising from inner Au core atoms and "initial state effect" arising from surface Au atoms.[32,75−79] Similarly, these two components could attribute to the shift of Pd($3d_{5/2}$ and $3d_{3/2}$) peaks for Pd NCs reported here. Due to the smaller sizes of these Pd NCs, the shift could most probably be influenced by the "initial state effect." The comparison of Pd 3d core-level spectra of dark and yellow bands (Figure S3) showing similar binding energy further confirms that the monotonic shift is observed from Pd NCs. Another important observation is the absence of satellite peaks. The good match of the observed spectra with preliminary data fitting (blue dotted line in Figure 4(inset)) and the absence of satellite peaks eliminates the possibility of other charge states of Pd present in the sample.[72,73,80,81]

CONCLUSIONS

In summary, we demonstrated that the two-phase Brust synthesis can be utilized to synthesize atomically precise Pd

https://doi.org/10.1021/acs.jpcc.1c09453
J. Phys. Chem. C 2022, 126, 444−450

NCs using phenylethanethiol. The composition of new Pd NCs is $Pd_{21}(SCH_2CH_2Ph)_{18}$ and $Pd_{38}(SCH_2CH_2Ph)_{21}S_2$. This composition is unequivocally confirmed by isotopically resolved ESI-MS. The size distribution is confirmed using MALDI-MS. The XPS spectrum reiterates the cluster formation and the size of these Pd NCs.

■ ASSOCIATED CONTENT

Supporting Information

The Supporting Information is available free of charge at https://pubs.acs.org/doi/10.1021/acs.jpcc.1c09453.

XPS data of carbon and sulfide, ESI-MS spectra comparison, and XPS spectra comparison of dark and yellow bands (PDF)

■ AUTHOR INFORMATION

Corresponding Author

Amala Dass − *Department of Chemistry and Biochemistry, University of Mississippi, Oxford, Mississippi 38677, United States;* orcid.org/0000-0001-6942-5451; Email: amal@olemiss.edu

Author

Senthil Kumar Eswaramoorthy − *Department of Chemistry and Biochemistry, University of Mississippi, Oxford, Mississippi 38677, United States;* orcid.org/0000-0001-8015-1391

Complete contact information is available at: https://pubs.acs.org/10.1021/acs.jpcc.1c09453

Notes

The authors declare no competing financial interest.

■ ACKNOWLEDGMENTS

NSF-CHE-1808138 supported the performed work. The authors acknowledge Dr. Felio Perez and Integrated Microscopy Center at The University of Memphis for the support in XPS data collection.

■ REFERENCES

(1) Alvarez, M. M.; Khoury, J. T.; Schaaff, T. G.; Shafigullin, M. N.; Vezmar, I.; Whetten, R. L. Optical Absorption Spectra of Nanocrystal Gold Molecules. *J. Phys. Chem. B* **1997**, *101*, 3706−3712.

(2) Schaaff, T. G.; Shafigullin, M. N.; Khoury, J. T.; Vezmar, I.; Whetten, R. L.; Cullen, W. G.; First, P. N.; Gutiérrez-Wing, C.; Ascensio, J.; Jose-Yacamán, M. J. Isolation of Smaller Nanocrystal Au Molecules: Robust Quantum Effects in Optical Spectra. *J. Phys. Chem. B* **1997**, *101*, 7885−7891.

(3) Maity, P.; Xie, S.; Yamauchi, M.; Tsukuda, T. Stabilized gold clusters: from isolation toward controlled synthesis. *Nanoscale* **2012**, *4*, 4027−4037.

(4) Whetten, R. L.; Khoury, J. T.; Alvarez, M. M.; Murthy, S.; Vezmar, I.; Wang, Z. L.; Stephens, P. W.; Cleveland, C. L.; Luedtke, W. D.; Landman, U. Nanocrystal gold molecules. *Adv. Mater.* **1996**, *8*, 428−433.

(5) Schaaff, T. G.; Shafigullin, M. N.; Khoury, J. T.; Vezmar, I.; Whetten, R. L. Properties of a Ubiquitous 29 kDa Au:SR Cluster Compound. *J. Phys. Chem. B* **2001**, *105*, 8785−8796.

(6) Schaaff, T. G.; Whetten, R. L. Controlled Etching of Au:SR Cluster Compounds. *J. Phys. Chem. B* **1999**, *103*, 9394−9396.

(7) Chakraborty, I.; Pradeep, T. Atomically Precise Clusters of Noble Metals: Emerging Link between Atoms and Nanoparticles. *Chem. Rev.* **2017**, *117*, 8208−8271.

(8) Udayabhaskararao, T.; Pradeep, T. New Protocols for the Synthesis of Stable Ag and Au Nanocluster Molecules. *J. Phys. Chem. Lett.* **2013**, *4*, 1553−1564.

(9) Antonello, S.; Hesari, M.; Polo, F.; Maran, F. Electron transfer catalysis with monolayer protected Au25 clusters. *Nanoscale* **2012**, *4*, 5333−5342.

(10) Aiken, J. D.; Finke, R. G. A review of modern transition-metal nanoclusters: their synthesis, characterization, and applications in catalysis. *J. Mol. Catal. A: Chem.* **1999**, *145*, 1−44.

(11) Love, J. C.; Estroff, L. A.; Kriebel, J. K.; Nuzzo, R. G.; Whitesides, G. M. Self-Assembled Monolayers of Thiolates on Metals as a Form of Nanotechnology. *Chem. Rev.* **2005**, *105*, 1103−1170.

(12) Abbas, M. A.; Kim, T.-Y.; Lee, S. U.; Kang, Y. S.; Bang, J. H. Exploring Interfacial Events in Gold-Nanocluster-Sensitized Solar Cells: Insights into the Effects of the Cluster Size and Electrolyte on Solar Cell Performance. *J. Am. Chem. Soc.* **2016**, *138*, 390−401.

(13) Hartland, G. V. Optical Studies of Dynamics in Noble Metal Nanostructures. *Chem. Rev.* **2011**, *111*, 3858−3887.

(14) Zhang, X.-D.; Chen, J.; Luo, Z.; Wu, D.; Shen, X.; Song, S.-S.; Sun, Y.-M.; Liu, P.-X.; Zhao, J.; Huo, S.; et al. Enhanced Tumor Accumulation of Sub-2 nm Gold Nanoclusters for Cancer Radiation Therapy. *Adv. Healthcare Mater.* **2014**, *3*, 133−141.

(15) Zhang, X.-D.; Luo, Z.; Chen, J.; Shen, X.; Song, S.; Sun, Y.; Fan, S.; Fan, F.; Leong, D. T.; Xie, J. Ultrasmall Au10−12(SG)10−12 Nanomolecules for High Tumor Specificity and Cancer Radiotherapy. *Adv. Mater.* **2014**, *26*, 4565−4568.

(16) Fang, J.; Zhang, B.; Yao, Q.; Yang, Y.; Xie, J.; Yan, N. Recent advances in the synthesis and catalytic applications of ligand-protected, atomically precise metal nanoclusters. *Coord. Chem. Rev.* **2016**, *322*, 1−29.

(17) Niihori, Y.; Yoshida, K.; Hossain, S.; Kurashige, W.; Negishi, Y. Deepening the Understanding of Thiolate-Protected Metal Clusters Using High-Performance Liquid Chromatography. *Bull. Chem. Soc. Jpn.* **2019**, *92*, 664−695.

(18) Cheng, H.; Wang, X.; Liu, X.; Wang, X.; Wen, H.; Cheng, Y.; Xie, A.; Shen, Y.; Tang, R.; Zhu, M. An effective NIR laser/tumor-microenvironment co-responsive cancer theranostic nanoplatform with multi-modal imaging and therapies. *Nanoscale* **2021**, *13*, 10816−10828.

(19) Alvarez, M. M.; Khoury, J. T.; Schaaff, T. G.; Shafigullin, M.; Vezmar, I.; Whetten, R. L. Critical sizes in the growth of Au clusters. *Chem. Phys. Lett.* **1997**, *266*, 91−98.

(20) Balasubramanian, R.; Guo, R.; Mills, A. J.; Murray, R. W. Reaction of Au55(PPh3)12Cl6 with Thiols Yields Thiolate Monolayer Protected Au75 Clusters. *J. Am. Chem. Soc.* **2005**, *127*, 8126−8132.

(21) Jimenez, V. L.; Georganopoulou, D. G.; White, R. J.; Harper, A. S.; Mills, A. J.; Lee, D.; Murray, R. W. Hexanethiolate Monolayer Protected 38 Gold Atom Cluster. *Langmuir* **2004**, *20*, 6864−6870.

(22) Schaaff, T. G.; Knight, G.; Shafigullin, M. N.; Borkman, R. F.; Whetten, R. L. Isolation and Selected Properties of a 10.4 kDa Gold:Glutathione Cluster Compound. *J. Phys. Chem. B* **1998**, *102*, 10643−10646.

(23) Schaaff, T. G.; Whetten, R. L. Giant Gold−Glutathione Cluster Compounds: Intense Optical Activity in Metal-Based Transitions. *J. Phys. Chem. B* **2000**, *104*, 2630−2641.

(24) Gutiérrez, E.; Powell, R. D.; Furuya, F. R.; Hainfeld, J. F.; Schaaff, T. G.; Shafigullin, M. N.; Stephens, P. W.; Whetten, R. L. Greengold, a giant cluster compound of unusual electronic structure. *Eur. Phys. J. D* **1999**, *9*, 647−651.

(25) Dass, A.; Stevenson, A.; Dubay, G. R.; Tracy, J. B.; Murray, R. W. Nanoparticle MALDI-TOF Mass Spectrometry without Fragmentation: Au25(SCH2CH2Ph)18 and Mixed Monolayer Au25-(SCH2CH2Ph)18−x(L)x. *J. Am. Chem. Soc.* **2008**, *130*, 5940−5946.

(26) Dole, M.; Mack, L. L.; Hines, R. L.; Mobley, R. C.; Ferguson, L. D.; Alice, M. B. Molecular Beams of Macroions. *J. Chem. Phys.* **1968**, *49*, 2240−2249.

(27) Yamashita, M.; Fenn, J. B. Electrospray ion source. Another variation on the free-jet theme. *J. Phys. Chem. A* **1984**, *88*, 4451−4459.
(28) Tracy, J. B.; Kalyuzhny, G.; Crowe, M. C.; Balasubramanian, R.; Choi, J.-P.; Murray, R. W. Poly(ethylene glycol) Ligands for High-Resolution Nanoparticle Mass Spectrometry. *J. Am. Chem. Soc.* **2007**, *129*, 6706−6707.
(29) Comby-Zerbino, C.; Dagany, X.; Chirot, F.; Dugourd, P.; Antoine, R. The emergence of mass spectrometry for characterizing nanomaterials. Atomically precise nanoclusters and beyond. *Mater. Adv.* **2021**, *2*, 4896−4913.
(30) Tracy, J. B.; Crowe, M. C.; Parker, J. F.; Hampe, O.; Fields-Zinna, C. A.; Dass, A.; Murray, R. W. Electrospray Ionization Mass Spectrometry of Uniform and Mixed Monolayer Nanoparticles: Au25[S(CH2)2Ph]18 and Au25[S(CH2)2Ph]18-x(SR)x. *J. Am. Chem. Soc.* **2007**, *129*, 16209−16215.
(31) Negishi, Y.; Takasugi, Y.; Sato, S.; Yao, H.; Kimura, K.; Tsukuda, T. Magic-Numbered Aun Clusters Protected by Glutathione Monolayers (n = 18, 21, 25, 28, 32, 39): Isolation and Spectroscopic Characterization. *J. Am. Chem. Soc.* **2004**, *126*, 6518−6519.
(32) Negishi, Y.; Nobusada, K.; Tsukuda, T. Glutathione-Protected Gold Clusters Revisited: Bridging the Gap between Gold(I)−Thiolate Complexes and Thiolate-Protected Gold Nanocrystals. *J. Am. Chem. Soc.* **2005**, *127*, 5261−5270.
(33) Shichibu, Y.; Negishi, Y.; Tsukuda, T.; Teranishi, T. Large-Scale Synthesis of Thiolated Au25 Clusters via Ligand Exchange Reactions of Phosphine-Stabilized Au11 Clusters. *J. Am. Chem. Soc.* **2005**, *127*, 13464−13465.
(34) Negishi, Y.; Takasugi, Y.; Sato, S.; Yao, H.; Kimura, K.; Tsukuda, T. Kinetic Stabilization of Growing Gold Clusters by Passivation with Thiolates. *J. Phys. Chem. B* **2006**, *110*, 12218−12221.
(35) Heaven, M. W.; Dass, A.; White, P. S.; Holt, K. M.; Murray, R. W. Crystal Structure of the Gold Nanoparticle [N(C8H17)4][Au25-(SCH2CH2Ph)18]. *J. Am. Chem. Soc.* **2008**, *130*, 3754−3755.
(36) Udaya Bhaskara Rao, T.; Pradeep, T. Luminescent Ag7 and Ag8 Clusters by Interfacial Synthesis. *Angew. Chem., Int. Ed.* **2010**, *49*, 3925−3929.
(37) Khatun, E.; Pradeep, T. New Routes for Multicomponent Atomically Precise Metal Nanoclusters. *ACS Omega* **2021**, *6*, 1−16.
(38) Xie, J.; Lee, J. Y.; Wang, D. I. C.; Ting, Y. P. Silver Nanoplates: From Biological to Biomimetic Synthesis. *ACS Nano* **2007**, *1*, 429−439.
(39) Yuan, X.; Tay, Y.; Dou, X.; Luo, Z.; Leong, D. T.; Xie, J. Glutathione-Protected Silver Nanoclusters as Cysteine-Selective Fluorometric and Colorimetric Probe. *Anal. Chem.* **2013**, *85*, 1913−1919.
(40) Yao, Q.; Chen, T.; Yuan, X.; Xie, J. Toward Total Synthesis of Thiolate-Protected Metal Nanoclusters. *Acc. Chem. Res.* **2018**, *51*, 1338−1348.
(41) Zhou, M.; Bao, Y.; Jin, S.; Wen, S.; Chen, S.; Zhu, M. [Ag71(S-tBu)31(Dppm)](SbF6)2: an intermediate-sized metalloid silver nanocluster containing a building block of Ag64. *Chem. Commun.* **2021**, *57*, 10383−10386.
(42) Ma, X.; Bai, Y.; Song, Y.; Li, Q.; Lv, Y.; Zhang, H.; Yu, H.; Zhu, M. Rhombicuboctahedral Ag100: Four-Layered Octahedral Silver Nanocluster Adopting the Russian Nesting Doll Model. *Angew. Chem., Int. Ed.* **2020**, *59*, 17234−17238.
(43) Baghdasaryan, A.; Bürgi, T. Copper nanoclusters: designed synthesis, structural diversity, and multiplatform applications. *Nanoscale* **2021**, *13*, 6283−6340.
(44) Li, H.; Zhai, H.; Zhou, C.; Song, Y.; Ke, F.; Xu, W. W.; Zhu, M. Atomically Precise Copper Cluster with Intensely Near-Infrared Luminescence and Its Mechanism. *J. Phys. Chem. Lett.* **2020**, *11*, 4891−4896.
(45) Tsuji, J. *Palladium Reagents and Catalysts: Innovations in Organic Synthesis*; Wiley & Sons: Chichester; New York, 2002.
(46) Tsuji, J. Palladium in Organic Synthesis, 2005.
(47) Lu, C.-H.; Chang, F.-C. Polyhedral Oligomeric Silsesquioxane-Encapsulating Amorphous Palladium Nanoclusters as Catalysts for Heck Reactions. *ACS Catal.* **2011**, *1*, 481−488.
(48) Cargnello, M.; Wieder, N. L.; Canton, P.; Montini, T.; Giambastiani, G.; Benedetti, A.; Gorte, R. J.; Fornasiero, P. A Versatile Approach to the Synthesis of Functionalized Thiol-Protected Palladium Nanoparticles. *Chem. Mater.* **2011**, *23*, 3961−3969.
(49) Mednikov, E. G.; Dahl, L. F. Palladium: It Forms Unique Nano-Sized Carbonyl Clusters. *J. Chem. Educ.* **2009**, *86*, No. 1135.
(50) Mednikov, E. G.; Jewell, M. C.; Dahl, L. F. Nanosized (μ12-Pt)Pd164-xPtx(CO)72(PPh3)20 (x ≈ 7) Containing Pt-Centered Four-Shell 165-Atom Pd−Pt Core with Unprecedented Intershell Bridging Carbonyl Ligands: Comparative Analysis of Icosahedral Shell-Growth Patterns with Geometrically Related Pd145(CO)x-(PEt3)30 (x ≈ 60) Containing Capped Three-Shell Pd145 Core. *J. Am. Chem. Soc.* **2007**, *129*, 11619−11630.
(51) Teramoto, M.; Iwata, K.; Yamaura, H.; Kurashima, K.; Miyazawa, K.; Kurashige, Y.; Yamamoto, K.; Murahashi, T. Three-Dimensional Sandwich Nanocubes Composed of 13-Atom Palladium Core and Hexakis-Carbocycle Shell. *J. Am. Chem. Soc.* **2018**, *140*, 12682−12686.
(52) Marshall, S. T.; O'Brien, M.; Oetter, B.; Corpuz, A.; Richards, R. M.; Schwartz, D. K.; Medlin, J. W. Controlled selectivity for palladium catalysts using self-assembled monolayers. *Nat. Mater.* **2010**, *9*, 853−858.
(53) Zhao, S.; Zhang, H.; House, S. D.; Jin, R.; Yang, J. C.; Jin, R. Ultrasmall Palladium Nanoclusters as Effective Catalyst for Oxygen Reduction Reaction. *ChemElectroChem* **2016**, *3*, 1225−1229.
(54) Negishi, Y.; Murayama, H.; Tsukuda, T. Formation of Pdn(SR)m clusters (n<60) in the reactions of PdCl2 and RSH (R=n-C18H37, n-C12H25). *Chem. Phys. Lett.* **2002**, *366*, 561−566.
(55) Zhang, L.; Hu, Q.; Li, Z.; Zhang, Y.; Lu, D.; Shuang, S.; Choi, M. M. F.; Dong, C. Chromatographic separation and mass spectrometric analysis of N-acetyl-l-cysteine-protected palladium nanoparticles. *Anal. Methods* **2017**, *9*, 4539−4546.
(56) Chen, J.; Liu, L.; Weng, L.; Lin, Y.; Liao, L.; Wang, C.; Yang, J.; Wu, Z. Synthesis and Properties Evolution of a Family of Tiara-like Phenylethanethiolated Palladium Nanoclusters. *Sci. Rep.* **2015**, *5*, No. 16628.
(57) Stash, A. I.; Perepelkova, T. I.; Noskov, Y. G.; Buslaeva, T. M.; Romm, I. P. Palladium Clusters Pd4(SEt)4(OAc)4and Pd6(SEt)12: Structure and Properties. *Russ. J. Coord. Chem.* **2001**, *27*, 585−590.
(58) Yang, Z.; Smetana, A. B.; Sorensen, C. M.; Klabunde, K. J. Synthesis and Characterization of a New Tiara Pd(II) Thiolate Complex, [Pd(SC12H25)2]6, and Its Solution-Phase Thermolysis to Prepare Nearly Monodisperse Palladium Sulfide Nanoparticles. *Inorg. Chem.* **2007**, *46*, 2427−2431.
(59) Yang, Z.; Klabunde, K. J.; Sorensen, C. M. From Monodisperse Sulfurized Palladium Nanoparticles to Tiara Pd(II) Thiolate Clusters: Influence of Thiol Ligand on Thermal Treatment of a Palladium(II)−Amine System. *J. Phys. Chem. C* **2007**, *111*, 18143−18147.
(60) Gao, X.; Chen, W. Highly stable and efficient Pd6(SR)12 cluster catalysts for the hydrogen and oxygen evolution reactions. *Chem. Commun.* **2017**, *53*, 9733−9736.
(61) Nobusada, K.; Yamaki, T. Electronic Properties of Palladium−Thiolate Complexes with Tiara-like Structures. *J. Phys. Chem. A* **2004**, *108*, 1813−1817.
(62) Chen, J.; Liu, L.; Liu, X.; Liao, L.; Zhuang, S.; Zhou, S.; Yang, J.; Wu, Z. Gold-Doping of Double-Crown Pd Nanoclusters. *Chem. - Eur. J.* **2017**, *23*, 18187−18192.
(63) Yun, Y.; Sheng, H.; Yu, J.; Bao, L.; Du, Y.; Xu, F.; Yu, H.; Li, P.; Zhu, M. Boosting the Activity of Ligand-on Atomically Precise Pd3Cl Cluster Catalyst by Metal-Support Interaction from Kinetic and Thermodynamic Aspects. *Adv. Synth. Catal.* **2018**, *360*, 4731−4743.
(64) Corthey, G.; Rubert, A. A.; Picone, A. L.; Casillas, G.; Giovanetti, L. J.; Ramallo-López, J. M.; Zelaya, E.; Benitez, G. A.; Requejo, F. G.; José-Yacamán, M.; et al. New Insights into the Chemistry of Thiolate-Protected Palladium Nanoparticles. *J. Phys. Chem. C* **2012**, *116*, 9830−9837.

https://doi.org/10.1021/acs.jpcc.1c09453
J. Phys. Chem. C 2022, 126, 444−450

(65) Brust, M.; Walker, M.; Bethell, D.; Schiffrin, D. J.; Whyman, R. Synthesis of thiol-derivatised gold nanoparticles in a two-phase Liquid−Liquid system. *J. Chem. Soc., Chem. Commun.* **1994**, 801−802.
(66) Sakthivel, N. A.; Jupally, V. R.; Eswaramoorthy, S. K.; Wijesinghe, K. H.; Nimmala, P. R.; Kumara, C.; Rambukwella, M.; Jones, T.; Dass, A. Size Exclusion Chromatography: An Indispensable Tool for the Isolation of Monodisperse Gold Nanomolecules. *Anal. Chem.* **2021**, *93*, 3987−3996.
(67) Crasto, D.; Malola, S.; Brosofsky, G.; Dass, A.; Häkkinen, H. Single Crystal XRD Structure and Theoretical Analysis of the Chiral Au30S(S-t-Bu)18 Cluster. *J. Am. Chem. Soc.* **2014**, *136*, 5000−5005.
(68) Murayama, H.; Ichikuni, N.; Negishi, Y.; Nagata, T.; Tsukuda, T. EXAFS study on interfacial structure between Pd cluster and n-octadecanethiolate monolayer: formation of mixed Pd−S interlayer. *Chem. Phys. Lett.* **2003**, *376*, 26−32.
(69) Love, J. C.; Wolfe, D. B.; Haasch, R.; Chabinyc, M. L.; Paul, K. E.; Whitesides, G. M.; Nuzzo, R. G. Formation and Structure of Self-Assembled Monolayers of Alkanethiolates on Palladium. *J. Am. Chem. Soc.* **2003**, *125*, 2597−2609.
(70) Love, J. C.; Wolfe, D. B.; Chabinyc, M. L.; Paul, K. E.; Whitesides, G. M. Self-Assembled Monolayers of Alkanethiolates on Palladium Are Good Etch Resists. *J. Am. Chem. Soc.* **2002**, *124*, 1576−1577.
(71) Sakai, N.; Tatsuma, T. One-step synthesis of glutathione-protected metal (Au, Ag, Cu, Pd, and Pt) cluster powders. *J. Mater. Chem. A* **2013**, *1*, 5915−5922.
(72) Choudary, B. M.; Kumar, K. R.; Jamil, Z.; Thyagarajan, G. A novel 'anchored' palladium(II) phosphinated montmorillonite: the first example in the interlamellars of smectite clay. *J. Chem. Soc., Chem. Commun.* **1985**, 931−932.
(73) Kumar, G.; Blackburn, J. R.; Albridge, R. G.; Moddeman, W. E.; Jones, M. M. Photoelectron spectroscopy of coordination compounds. II. Palladium complexes. *Inorg. Chem.* **1972**, *11*, 296−300.
(74) Sleigh, C.; Pijpers, A. P.; Jaspers, A.; Coussens, B.; Meier, R. J. On the determination of atomic charge via ESCA including application to organometallics. *J. Electron Spectrosc. Relat. Phenom.* **1996**, *77*, 41−57.
(75) Zhang, P.; Sham, T. K. X-Ray Studies of the Structure and Electronic Behavior of Alkanethiolate-Capped Gold Nanoparticles: The Interplay of Size and Surface Effects. *Phys. Rev. Lett.* **2003**, *90*, No. 245502.
(76) Moriarty, P. Comment on "X-Ray Studies of the Structure and Electronic Behavior of Alkanethiolate-Capped Gold Nanoparticles: The Interplay of Size and Surface Effects". *Phys. Rev. Lett.* **2004**, *92*, No. 109601.
(77) Zhang, P.; Sham, T. K. Zhang and Sham Reply. *Phys. Rev. Lett.* **2004**, *92*, No. 109602.
(78) Tanaka, A.; Takeda, Y.; Imamura, M.; Sato, S. Dynamic final-state effect on the Au 4f core-level photoemission of dodecanethiolate-passivated Au nanoparticles on graphite substrates. *Phys. Rev. B* **2003**, *68*, No. 195415.
(79) Tanaka, A.; Takeda, Y.; Nagasawa, T.; Takahashi, K. Chemical states of dodecanethiolate-passivated Au nanoparticles: synchrotron-radiation photoelectron spectroscopy. *Solid State Commun.* **2003**, *126*, 191−196.
(80) Ghijsen, J.; Tjeng, L. H.; van Elp, J.; Eskes, H.; Westerink, J.; Sawatzky, G. A.; Czyzyk, M. T. Electronic structure of Cu2O and CuO. *Phys. Rev. B* **1988**, *38*, 11322−11330.
(81) Ganguly, A.; Chakraborty, I.; Udayabhaskararao, T.; Pradeep, T. A copper cluster protected with phenylethanethiol. *J. Nanopart. Res.* **2013**, *15*, No. 1522.

https://doi.org/10.1021/acs.jpcc.1c09453
J. Phys. Chem. C 2022, 126, 444−450